Performance Analysis of Time Synchronization Protocols in Wireless Sensor Networks with Regular Topologies

José A. Sánchez Fernández, José F. Martínez Ortega, Ana B. García Hernando, Lourdes López Santidrián
Dpto. de Ingeniería y Arquitecturas Telemáticas. E.U.I.T. de Telecomunicación
Universidad Politécnica de Madrid
Campus Sur UPM. Cta. de Valencia, km.7. 28031 Madrid, Spain
e-mail: {jsanchez, jfmartin, abgarcia, llopez}@diatel.upm.es

***Abstract*— Time synchronization in wireless sensor networks is an essential issue in their operation. The synchronization is deeply influenced by network size and complexity. System dynamics and algebraic graph theory provide the suitable mathematical framework to describe the dynamical and topological features of complex networks. These features are very useful to understand overall aspects of network time evolution, in particular the ability to achieve steady synchronization states. In this paper, we apply the mathematical tools provided by theory to assess the ease of synchronization of a wireless sensor network with regular topology, initially designed to support surveillance applications. From these theoretical results, the research work described will focus on the performance analysis of different time synchronization protocols that allow network nodes to share a common global time, either with the diffusion of a master reference timestamp or with the consecutive exchange of local timestamps among neighbor nodes, in order to achieve a global dynamical consensus.**

Keywords— wireless sensor network; synchonization protocol; spectral graph theory; consensus dynamics; surveillance application.

I. INTRODUCTION

For numerous wireless sensor network (WSN) applications, e.g., localization, security or surveillance, where event detection and reporting is a usual task, time synchronization is a major issue. Different sources of unreliability, and also the complexity and size of the WSN affect the performance of different synchronization methods. Certain knowledge of the mathematical models proposed for the analysis of complex networks is needed to understand and solve the underlying problems that could arise. Also, these models provide a good assistance in the design of reliable synchronization protocols.

These mathematical models are directly inspired by those historically developed for complex biological, chemical or physical systems, which can be described in terms of interactions among mutually coupled oscillators. A dynamical analysis of many of these systems reveals important analogies regarding WSN performance, since the time evolution of a single sensor, acting as a node of the whole network, can be modeled as a simple oscillator interacting with the physical environment and the rest of the network.

System Dynamics provide the description of time evolution of the state variables of nodes, reporting useful information about the stability of the network states, while Algebraic Graph Theory is a valuable help to visualize the topology of the network. The study of values of some graph invariants, e.g., the eigenvalues of matrices that describe the connections among network nodes, is very useful to understand the conditions of synchronizability of the whole network. The main purpose of this paper is to apply some of these mathematical tools to a specific WSN with regular topology, initially designed to support surveillance applications; these results will establish the synchronization ability of the network topology chosen. As a extension of [1], alternative synchronization methods will be tested and compared.

The outline of the paper is given as follows. Section II summarizes main theoretical research done about synchronization of complex networks composed of coupled oscillators. Section III describes the approximation to physical time made by hardware oscillators in WSN nodes. Section IV introduces the mathematical model that describes the evolution of a network composed of mutually coupled oscillators, and some basic concepts of Algebraic Graph Theory, which are needed in the analysis of time synchronization. Section V presents the generic results that establish the conditions to reach the synchronization in a complex network. Section VI shows the surveillance application domain, the underlying WSN and the requirements of its synchronization. Section VII discusses the results provided by the application of the mathematical models to state the conditions of a better synchronization for the WSN. Section VIII shows the performance of different synchronization methods on the scenario described above. Finally, Section IX summarizes the conclusions and provides ideas for possible future works.

II. LITERATURE SURVEY

Historically, different but related mathematical models have been proposed to study the synchronization of complex systems, which are described through networks composed of coupled oscillators. Some of the main references in this research field are discussed next. Mirollo, Watts and Strogatz studied the spontaneous synchronizability of biological systems composed of globally coupled identical oscillators [2][3], showing the conditions that lead to the stability of the

synchronization state. They analyzed the influence of the traditionally called "small-world effect" on network synchronization, i.e., the addition of some random links to regular lattices, acting as a kind of shortcut connection, enhance the synchronization capabilities of the network.

Chemical systems were studied by Kuramoto [4], who proposed a mathematical model for arbitrary nonlinear phase-coupled oscillators; he showed that the ability to reach a synchronization state relies on the coupling strength among oscillators. Barahona and Pecora studied the synchronization of complex networks composed of identical oscillators through a linear model [5][6], and they showed the strong dependence of the synchronization state to some topological parameters. Barbarossa, Celano and Scutari proposed an extension of the Kuramoto model applied to WSN [7][8][9], which is designed as a system composed of phase-coupled oscillators with nonlinear coupling. They studied the application of distributed synchronization algorithms, and also they showed the impact of synchronization in network overall energy consumption.

In these models, each network node, e.g., a network device including some sensors that collect data from its physical environment, is characterized by a set of state variables. Time evolution of these variables, and coupling interactions among nodes, are described by a system of differential equations. The whole network is modeled with a graph, which includes the information about network topology, basically the existence of communication links between each pair of nodes.

Since the graph is constructed by a set of matrices (adjacency, incidence and laplacian matrices), it is possible to apply Algebraic Graph Theory, a well established field of Discrete Mathematics [10][11][12][13]. Results obtained establish the requirements of synchronizability of the whole network. These requirements rely on a set of inequalities, connecting different parameters, strongly dependent on the overall topology of the network [6][14].

These models are the formal basis in the development of synchronization protocols for WSN. Several proposals have been done, and excellent surveys about this topic have been previously published [15][19]. These surveys present pertinent remarks about challenges and constraints in synchronization protocol design. Also, they include exhaustive classifications of protocols, based on clock models used (constant frequency, bounded frequency deviation, drift-constraint) [16][17][18][19], synchronization classes (external vs. internal, probabilistic vs. deterministic, permanent vs. by request, complete vs. partial) [15][16][19], synchronization techniques (unilateral, bilateral, cyclic, by broadcast correction) [16][17][19], and models of interaction among network nodes (unicast vs. multicast, symmetric vs. asymmetric, explicit vs. implicit) [15][16][19]. Critics of features and performance of the synchronization protocols proposed are also included. It is not aim of this brief summary to discuss these details; the reader interested in these topics is encouraged to address to the above references.

The research work described in this paper focuses on synchronization methods that allow network nodes to share a common global time, either with the diffusion of a master reference timestamp or with the consecutive exchange of local timestamps among neighbor nodes, in order to achieve a global dynamical consensus. These approaches are adopted in some proposals, e.g., [8][20][21]. The synchronization algorithms will be applied to a static WSN with a selected regular topology. Next two sections will focus on the description of formal expression of the time measured by a WSN, and also on the mathematical models proposed to study the time synchronization.

III. PHYSICAL TIME AND PHYSICAL CLOCKS

First of all, it will be appropriate to describe the way that the measurement of physical time is made by WSN nodes. This estimation must be coherent with the mathematical model introduced later, in Section IV.

In a WSN, its nodes are usually equipped with a computer clock assisted by a hardware oscillator. Every node i (i= 1,…, N) implements a local approximation $x_i(t)$ to an external source of physical time t, e.g., based on Universal Time Coordinated (UTC) [16][19]. The approximation can be expressed as a function $x_i(t)$: $\mathbb{R} \rightarrow \mathbb{R}$, which is

$$x_i(t) = x_i(0) + K\int_0^t \omega(\tau)d\tau. \quad (1)$$

This function depends on the oscillator frequency, $\boldsymbol{\omega}(t)$, and of a scale constant, K. Initially, $\boldsymbol{\omega}(t)$ is supposed to be equivalent in all nodes. $x_i(t)$ is recorded in a register, which is updated through the oscillator interrupt cycles. The clock accuracy, and therefore its energy consumption, are proportional to the frequency $\boldsymbol{\omega}$.

Ideally, with an appropriate selection of K and $\boldsymbol{\omega}(t)$, $x_i(t) = t$. However, there are unavoidable sources of error, which are due, mainly, to a limited accuracy of hardware clocks, and also to instabilities of the physical environment. Variations of physical magnitudes, e.g., temperature, or even internal changes in power supply can affect the performance of the clock. The clock absolute *offset* is defined as the difference $x_i(t) - t \neq 0$; the relative offset between two clocks is the difference $x_i(t) - x_j(t)$. The clock *skew* is the difference of its local frequency with respect to the external reference frequency, $\boldsymbol{\omega}(t) - \boldsymbol{\omega}_{ref}$; and the clock *drift* is the variation of this frequency, i.e., its derivative with respect to time, $\boldsymbol{\omega}'(t)$. Figure 1 shows the effects of clock skew and drift in real clocks.

These sources of inaccuracy induce a deviation of physical time recorded at the local clock of every WSN node with respect to the external time reference, and also with other local clocks. Usually, clock accuracy is reported in technical specifications of hardware clocks, given by the manufacturer [15][17]. So, although clock deviation cannot be completely removed, it can be properly bounded. If the required synchronization accuracy is small with respect to the cumulative effect due to frequency fluctuations, it is possible to assume that $\boldsymbol{\omega}(t)$ is approximately constant. If frequency fluctuations are not negligible but they are known, the bounds are given by the next inequalities [16][19]:

$$1-\rho \le \frac{dx_i(t)}{dt} \le 1+\rho, \quad (2)$$

where $\boldsymbol{\rho}$ is the maximum skew rate specified by the manufacturer. A clock never can stop or run backwards, so $\boldsymbol{\rho} > -1$. The effect of drift could be ignored if frequency fluctuations are small compared with the required synchronization accuracy. The presence or lack of these sources of error and related bounds establishes the clock model to deal with. Assuming the existence of clock skew and drift, $x_i(t)$ can be expanded by its Taylor series [17], in order to simplify the clock model, as

$$x_i(t) = \alpha_i + \beta_i t + \gamma_i t^2 + ... \quad (3)$$

So, the coefficient α_i can be associated with the initial offset of clock $x_i(t)$; the linear parameter, β_i, with the skew ($1 \pm \boldsymbol{\rho}$); and the quadratic parameter, γ_i, with a deviation from the linear behavior. These parameters can be estimated by statistical calculations. From (2) and (3), assuming a linear behavior in clocks, $x_i(t)$ can be bounded as

$$x_i(0) + (1-\rho)t \le x_i(t) \le x_i(0) + (1+\rho)t. \quad (4)$$

Finally, two clocks, $x_i(t)$ and $x_j(t)$, can be related to their relative offset, α_{ij}, and skew, β_{ij} [15], as

$$x_i(t) = \alpha_{ij} + \beta_{ij} x_j(t). \quad (5)$$

After consecutive requests and receptions of values of $x_j(t)$, node i can estimate the relative offset and skew with node j. Equation (5) can be extended to a group of connected nodes,

$$x_i(t) = \sum_{j \in N_i} (\alpha_{ij} + \beta_{ij} x_j(t)), \quad (6)$$

where N_i denotes the neighborhood of node i, i.e., the set of nodes connected to it. Since the difference between time records of any pair of nodes, $x_i(t) - x_j(t)$, trends to increase as t grows, the synchronization will try to cancel this difference, or, at least, to minimize it. The general formulation of the synchronization problem consists in a direct adjustment of the value $x_i(t)$ by the application of a synchronization algorithm. To proceed, each node must receive one or various packets containing external time references, and the algorithm should infer some additional estimations. Due to inaccuracies in the operation of WSN, some values need to be calculated ad hoc, e.g., the packet round trip time between different nodes, by timing exchanges of specific messages [15]. Other values, as the expected average delay in internal processing tasks, could be statistically or randomly estimated. Finally, the synchronization algorithm should not suppose a substantial overload to WSN operation. Next Section presents the dynamical model proposed to describe the behavior of complex networks. It will be shown that this formulation is consistent with the formal description of time measure given above.

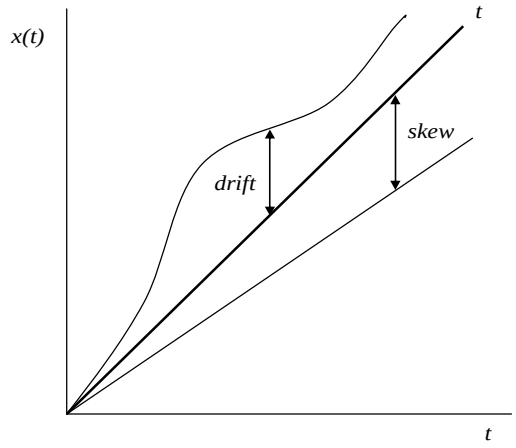

Figure 1. And ideal clock and two real clocks, with an initial offset equal to zero, and $x(0) = 0$. Effect of skew and drift shows, respectively, linear and nonlinear deviations from ideal reference time.

IV. WSN DYNAMICAL MODEL

Among the formal models proposed to describe complex network dynamics, the classical development of Barahona and Pecora has been selected [5][6], due to its generality and simplicity. This model considers a network composed of N nodes, each one including some sensors of the physical environment. The i-th node ($i = 1,\ldots,N$) takes different measures of M specific events, expressed by its state variable vector, $\boldsymbol{x}_i(t) = (x_{i1}(t),\ldots,x_{iM}(t))$.

The sensors act as mutually coupled oscillators, since they periodically communicate with other sensors falling into their coverage radius, sending and receiving some of the collected data or synchronization timestamps. Therefore, the nodes can adapt their state variables evolution according to data received from others, e.g., the time values of their clocks, to reach the synchronization.

The dynamical system present at each node evolves according to the following system of first order differential equations, as proposed in [6]:

$$\frac{d\boldsymbol{x}_i}{dt} = \boldsymbol{F}(x_i(t)) - \sigma \sum_{j=1}^{N} L_{ij} \boldsymbol{H}(x_j(t)), i = 1,..., N. \quad (7)$$

$\boldsymbol{F}(x_i(t))$ is a vector function of dimension M, that expresses the dynamics at each node, i.e., the evolution of its M state variables $\boldsymbol{x}_i(t)$, and σ is an overall coupling strength, supposed to be identical in all network nodes. The M-vector output function $\boldsymbol{H}(x_j(t))$ of the state variables of each oscillator represents the coupling among oscillators. Finally, L_{ij} are the components of a certain $N \times N$ connection matrix $\mathbf{L}$, which specifies the existing connections among nodes. $\mathbf{L}$ is symmetric, since it is assumed that the network nodes have nondirectional links.

Results obtained in [6] show the generic conditions that vector functions $\boldsymbol{F}(x_j(t))$, $\boldsymbol{H}(x_j(t))$, and matrix $\mathbf{L}$ must satisfy to reach an stable synchronization state in the network of

coupled oscillators whose dynamics is modeled by (7). It has been shown that this stability depends, mainly, on selected eigenvalues belonging to the spectrum of the connection matrix **L** [6]**,** which is invariant under permutations of network node labels. Therefore, it is essential to establish the elements L_{ij} of **L**.

To proceed, system of equations expressed in (7) can be conveniently simplified to facilitate the next analysis. It is possible to reduce the number of state variables in each node from *M* to 1, since the local time to be measured in each node from its internal hardware oscillator, $x_i(t)$, will be the only state variable to consider further. In that case, (7) gets a more familiar fashion:

$$\frac{dx_i}{dt} = K\omega(t) - \sigma\sum_{j=1}^{N} L_{ij}H(x_j(t)), \tag{8}$$

where $\boldsymbol{\omega}(t)$ represent the oscillation frequency, supposed to be identical in all nodes. It is interesting to note that, if coupling among nodes is nonexistent, the sum contained in the right member of (8) is equal to zero,

$$\sum_{j=1}^{N} L_{ij}H(x_j(t)) = 0, \tag{9}$$

and (8) is transformed in

$$\frac{dx_i}{dt} = K\omega(t), \tag{10}$$

which is formally equivalent to (1). Thus, the simplest case of dynamics at every node (nonexistent coupling) leads to the initial estimation of time made by network nodes. It could be considered as an argument of validity of the dynamical model presented above.

Once the network is synchronized, (8) must be identical for all the nodes. This is assured if the sum of its right member is constant:

$$\sum_{j=1}^{N} L_{ij}H(x_j(t)) = K. \tag{11}$$

In the simplest case, this sum is supposed null [6]. The connection matrix **L**, then, is restricted to have zero sum rows:

$$\sum_{j=1}^{N} L_{ij} = 0. \tag{12}$$

With this constraint, it is possible to obtain the elements L_{ij} of **L**. To that end, it will be useful to introduce before some basic concepts of Algebraic Graph Theory [10][11]. A network can be modeled by a graph $U=U(V,E)$ composed of *N* nodes or vertices *V*, labeled from 1 to *N*, and a set of connections or edges *E* among them. The number of edges can vary from 0 (no nodes are connected) to $N(N–1)/2$ (every node is connected with all the others). A graph is represented by its adjacency matrix **A**, a symmetric $N \times N$ matrix where $A_{ij} = 1$ if the nodes *i* and *j* are connected, and $A_{ij} = 0$ otherwise. Also, the components of its main diagonal are defined as $A_{ii} = 0$. The study of invariants of the adjacency matrix (i.e., its spectrum properties) has been widely studied [10][11].

The degree d_i of the node *i* is the sum of the number of edges connecting it to other nodes, which can be obtained from the sum of the values belonging to the *i*-th row of the adjacency matrix, i.e.,

$$\sum_{j=1}^{N} A_{ij} = d_i, \tag{13}$$

which suggests to form a new matrix **D,** called valency or degree matrix, whose main diagonal elements D_{ii} are equivalent to the *i*-th sums in (13). It is possible to build a new matrix, the laplacian matrix, as $\mathbf{L} = \mathbf{D} - \mathbf{A}$, which clearly fulfills the requirement derived from (12). The elements L_{ij} of **L**, at last, can be expressed as

$$L_{ij} = \delta_{ij}D_{ij} - A_{ij}. \tag{14}$$

Spectrum properties of **L** have been studied, as well [12, 13]; it would be useful to obtain its eigenvalues through analytical expressions, but, in general, this is not possible. The characteristic equation of **L**, $det(\mathbf{L} - \gamma\mathbf{1}) = 0$, gives a polynomial that is difficult to solve for large values of *N* (also, it is due to a strong dependence of eigenvalues with little variations of the polynomial coefficients).

However, cyclic graphs, associated with networks with ring topology, generate adjacency and laplacian matrices with circulant structure [6][11][12][22], whose eigenvalues are well known. In a circulant matrix, each row is a cyclic permutation of the first row. A ring network of *N* nodes, where each node is connected exclusively with its two neighbors, generates a cyclic graph called *cycle* ($\mathbf{C}_N$). In such graphs, adjacency and laplacian matrices adopt the next structure:

$$\mathbf{A}(\mathbf{C}_N) = \begin{pmatrix} 0 & 1 & 0 & \dots & 0 & 1 \\ 1 & 0 & 1 & \dots & 0 & 0 \\ 0 & 1 & 0 & \dots & 0 & 0 \\ \dots & \dots & \dots & \dots & \dots & \dots \\ 0 & 0 & 0 & \dots & 0 & 1 \\ 1 & 0 & 0 & \dots & 1 & 0 \end{pmatrix} \quad \mathbf{L}(\mathbf{C}_N) = \begin{pmatrix} 2 & -1 & 0 & \dots & 0 & -1 \\ -1 & 2 & -1 & \dots & 0 & 0 \\ 0 & -1 & 2 & \dots & 0 & 0 \\ \dots & \dots & \dots & \dots & \dots & \dots \\ 0 & 0 & 0 & \dots & 2 & -1 \\ -1 & 0 & 0 & \dots & -1 & 2 \end{pmatrix}$$

And eigenvalues of $\mathbf{L}(\mathbf{C}_N)$ are given by [6][22]

$$\gamma_i = 2\left(1 - \cos\frac{2\pi(i-1)}{N}\right). \tag{15}$$

In general, when a node is connected with its $2k$ neighbors, the resultant graph, known as *k*-cycle ($k\mathbf{C}_N$), gives the next Laplacian eigenvalues [6][22]:

$$\gamma_i = 2\left(k - \sum_{j=1}^{k} \cos\frac{2\pi(i-1)j}{N} \right). \quad (16)$$

Figure 2, adapted from [6], shows the eigenvalues of *k*-cycles, for $k = \{1,..,4\}$ and a network of $N = 100$ nodes. For N even, the graphics are symmetric from the ordinate line at $N/2 + 1$. For eack k, there are k local maximum values, and maximum degeneracy of eigenvalues is $2k$. The analytical expression for Laplacian eigenvalues has been shown for this regular topology. Section VI will show the importance of such a topology from the application domain point of view. Also, Section V will explore the relationship among eigenvalues of **L**, network topology and time synchronization.

Meanwhile, it will be suitable to study the synchronization convergence properties of (8). In the simplest coupling among nodes, the variation of $x_i(t)$ with time is a linear combination of its own value and the values $x_j(t)$ of the nodes connected to it. So, $H(x_j(t)) = x_j(t)$, and (8) is transformed in

$$\frac{dx_i}{dt} = -\sigma \sum_{j=1}^{N} L_{ij} x_j(t). \quad (17)$$

Introducing the definition of the elements L_{ij}, given in (14),

$$\frac{dx_i}{dt} = -\sigma \sum_{j=1}^{N} (\delta_{ij} D_{ij} - A_{ij}) = -\sigma \sum_{j \in N_i} (x_i(t) - x_j(t)), \quad (18)$$

where N_i denotes the neighborhood of node i. Equations (17) and (18) can be expressed in a more compact form,

$$\frac{d\boldsymbol{x}}{dt} = -\sigma \mathbf{L} \boldsymbol{x}(t). \quad (19)$$

This set of differential equations is known as *consensus dynamics* [9][23][24][25]. The state variable of each node evolves in time as a linear combination of its own state and the states of coupled nodes. If the state vector $\boldsymbol{x}(t)$ is initialized with the local measurement of time in nodes, $\boldsymbol{x}(0) = \boldsymbol{x}_0$, and the network is connected, $\boldsymbol{x}(t)$ converges to the average consensus vector

$$\boldsymbol{x}(t) \to \frac{1}{N} \boldsymbol{1}^T \boldsymbol{x}_0 \boldsymbol{1}. \quad (20)$$

where $\boldsymbol{1}^T = (1, 1, \ldots, 1)$. That is,

$$x_i(t) \to \frac{1}{N} \sum_{j=1}^{N} x_{0j}, \quad (21)$$

for $t \to \infty$.

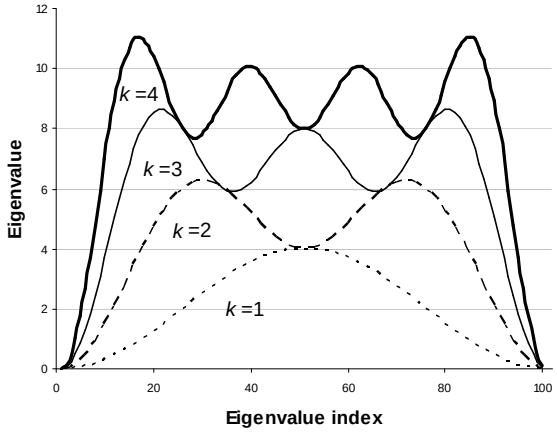

Figure 2. Eigenvalues of *k*-cycles for $k=\{1,2,3,4\}$ in a network of $N=100$ nodes (adapted from [6]). It is easy to visualize the simmetry of graphics from the ordinate line at $i = N/2 + 1$, the equivalence between the number of local maxima and k, the maximum degeneracy of eigenvalues, equal to $2k$, and the growth of maximum eigenvalues with k.

In other words, all local clocks converge to their initial average value, with independence of the coupling strength, σ. To visualize this convergence, (18) can be approximated with the next iterative expression:

$$x_{i,n+1} = x_{in} - \sigma \Delta t \sum_{j \in N_i} (x_{in} - x_{jn}). \quad (22)$$

In this approximation, n represents the n-th iteration step, and Δt is the interval of time elapsed between consecutive iterations. Figure 3 shows the convergence of (22), for a ring network example of $N = 5$ nodes, coupling strength $\sigma = 1$, interval time $\Delta t = 0{,}1$ sec., and exclusive coupling among nearest neighbor nodes. It is clearly shown that the local clocks converge to the constant average time value given in (21).

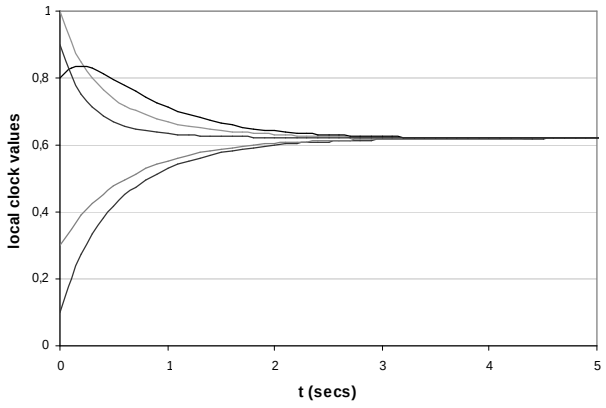

Figure 3. Consensus dynamics. Synchronization convergence example, in a ring network with $N = 5$ nodes, coupling strenght $\sigma = 1$, and interval time between succesive iterations $\Delta t = 0{,}1$ sec. At $t = 5$ secs., relative offset among clocks is $0{,}5 \times 10^{-3}$ sec.

To consider the increment of local clocks $x_j(t)$ with time, the frequency $\boldsymbol{\omega}$ must be taken into account, as follows,

$$\frac{dx_i}{dt} = K\omega - \sigma \sum_{j \in N_i} (x_i(t) - x_j(t)). \quad (23)$$

Synchronicity is acquired in a time varying form [23], and all the $x_i(t)$ converge to

$$x_i(t) \rightarrow \frac{1}{N} \sum_{j=1}^{N} K\omega t = K\omega t, \quad (24)$$

for $t \rightarrow \infty$**.** Adding the effect of frequency to the convergence steps expressed in (23), Figure 4 shows the convergence of this time-varying consensus dynamics, for the same type of network as above, with $K\boldsymbol{\omega}$ chosen to be 1, which gives a valid measure of time *t*, i.e., $x_i(t) \rightarrow t$.

Consensus dynamics, in both forms (constant or time varying), assures the stability of the global synchronization state. The time needed to get a full synchronicity is infinite, but in a real network the limited accuracy of local clocks influences the elapsed time to get a sufficient synchronization. This feature is present in different proposals of synchronization methods [8][9][21].

V. GENERIC CONDITIONS OF SYNCHRONIZABILITY FOR A WSN

This Section will use some results presented in [6][13] [14], very useful from the synchronization point of view, to extract generic conditions of synchronizability for a WSN.

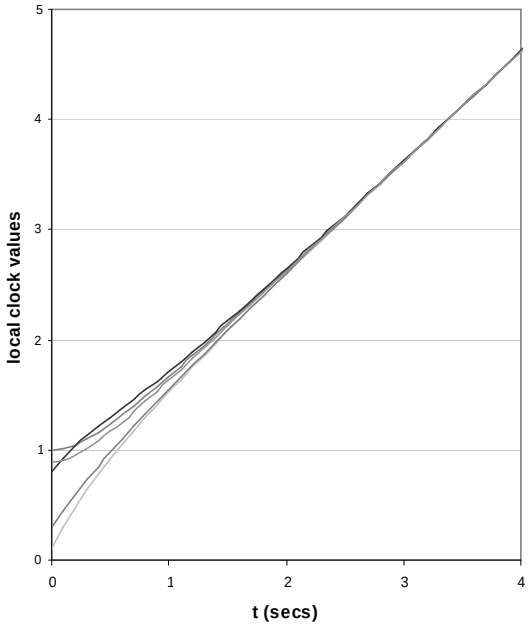

Figure 4. Time varying consensus dynamics. Synchronization convergence example. Ring network with N = 5 nodes, $\sigma = 1$, $\Delta t = 0{,}1$ sec, and $K\boldsymbol{\omega} = 1$. At $t = 4$ sec, relative offset among clocks is $0{,}2 \times 10^{-2}$sec. Convergence rate is independent of $\boldsymbol{\omega}$.

Laplacian matrix **L** is a positive, semi-definite matrix, with a maximum of *N* different nonnegative eigenvalues, γ_i, $1 \leq i \leq N$. They can be arranged in the sequence $\gamma_1 \leq \gamma_2 \leq \ldots \leq \gamma_M$, where $M \leq N$. By construction of **L**, its smaller eigenvalue, γ_1, is always zero, and it is associated with the eigenvector whose components are all equal to 1. The next larger eigenvalue, γ_2, is called algebraic connectivity, and is different from 0 if, and only if, the graph is connected. If γ_2 is close to 0, the graph can be easily split in subgraphs by the deletion of a few edges.

The algebraic connectivity, thus, plays a special role on the synchronizability of the network. Large values of γ_2 are associated with networks with a good connectivity among nodes, which improves the synchronization. On the other hand, if $\gamma_2 \rightarrow 0$, the network cannot reach synchronization easily. It has been shown that the synchronization time in the consensus dynamics context, given by (19), is proportional to γ_2^{-1} [25].

As it is noticed in [14], eigenvalue γ_2 by itself does not provide information about network topology. Nevertheless, some bounds for γ_2 have been found, which include the desired topological information. These bounds are expressed in the following set of inequalities [6][14]:

$$\gamma_2 \leq \frac{N}{N-1}\delta \leq \frac{N}{N-1}\Delta \leq \gamma_M \leq 2\Delta, \quad (25)$$

$$\frac{4}{ND} \leq \gamma_2 \leq \frac{Nd_i}{N-1}, \forall i, \quad (26)$$

where d_i is the degree of node *i*, δ is the minimum degree of the graph (the minimum value of the node degrees) and Δ is the maximum degree of the graph (the maximum value of the node degrees). The distance between two nodes, *i* and *j*, is defined as the minimum number of edges to traverse from node *i* to node *j*. The graph diameter, *D*, is the maximum value of distances. Networks with large values of *N* and *D* will give a small lower bound for γ_2. However, if these values are small, γ_2 will be greater and the network will synchronize better.

Also, the quotient γ_M/γ_2 should be as small as possible. The lowest value is 1, only possible if every node is connected with the rest of nodes. From (25) and (26), it can be shown [6][14] that

$$\frac{\Delta}{\delta} \leq \frac{\gamma_M}{\gamma_2}. \quad (27)$$

If the quotient γ_M/γ_2 is large (great difference between maximum and minimum degrees of the graph), the synchronization will be difficult. Maximum bounds for this quotient have been obtained [6][14]:

$$\frac{\gamma_M}{\gamma_2} \leq \frac{ND\Delta}{2} \quad (28)$$

Thus, if the values of maximum degree Δ, diameter *D* and number of nodes *N* can be reduced, the synchronizability

of the associated network will be enhanced. Finally, the average distance among nodes, l, can also give information about network synchronization properties [6][14]:

$$\frac{1}{\gamma_2} \leq \frac{(N-1)l}{2} - \frac{N-2}{4} \quad (29)$$

Networks with small number of nodes and small average distance generate a great value of γ_2, so they can be easily synchronized. Although there are some more bounds for γ_2 and γ_M, involving new topological parameters, e.g., isoperimetric number, clustering coefficient, and edge connectivity [14], the above inequalities show the essential approach to WSN synchronizability.

As conclusion, the combination of Network Dynamics and Algebraic Graph Theory provides useful tools to model a network and to obtain the conditions of its synchronization, which rely on overall network topological parameters. Next Section describes the specific surveillance application scenario of interest for this research, together with a justification on the importance that time synchronization plays in such a deployment.

VI. APPLICATION DOMAIN

One of the most important application types that can benefit from a WSN are those related to physical safety and watching of buildings or areas, i.e., surveillance applications. There is a wide range of related services, some of them applied to detect people and vehicle crossings on a virtual perimeter, and to warn about if need be. A network with regular ring topology is suitable to properly cover a virtual closed perimeter.

As part of the work inside the project µSWN (Solving Major Problems in Microsensorial Wireless Networks), financed by European Union VI Framework Program [26], a surveillance application of a closed virtual perimeter has been designed. The application is built through two different application agents, running on two different mote (WSN nodes) profiles, namely perimeter motes and bracelet motes. They will be designated perimeter agents and bracelet agents, respectively.

Perimeter motes are physically deployed covering a virtual perimeter. Some of these motes are equipped with one or two presence sensors (passive infrared sensors, PIR). Every hop between two neighbor perimeter motes is covered at least by one of these sensors. If someone crosses the perimeter, at least one of the PIR sensors detects it and triggers the activation of the corresponding perimeter agent or agents. Let us denote the area covered by the PIR sensors of node i as S_i. Let us also denote the position of a person crossing the perimeter as $\boldsymbol{r}_m$.

Whenever a crossing is signaled to a perimeter agent, i.e., $\exists\, i \,/\, \boldsymbol{r}_m \in S_i$, this agent tries to find out if the crossing has been caused by someone known or by an intruder. Known people (e.g., staff or authorized clients) wear a bracelet including a mote with a bracelet agent running, while of course intruders do not. Once the presence is known to the perimeter agent, it broadcasts to its neighbors (motes located inside its radio coverage) a specific message, which may include an identification of the PIR actually detecting the crossing or an identification of the node (if need be for the Surveillance algorithm). If a bracelet agent receives the message, it will answer to the enquirer providing its identifier. This identifier will be further forwarded by the perimeter agent to the sink, together with additional data, which may be significant for the algorithm running in the server. If no answer is received by the perimeter agent in a reasonable time, it is assumed that an intruder has crossed the perimeter. Therefore, this event is notified to the sink.

The fixed perimeter nodes and the mobile bracelets are equipped with omnidirectional antennas. Let R_i and R_m be the radio coverage areas of node n_i and of the mobile node, respectively, and let d_{mi} be the distance between n_i and the mobile node. If an unauthorized person crosses the perimeter, an intruder alert will be generated by all nodes n_i where $\boldsymbol{r}_m \in S_i$. If an authorized person (i.e., a person carrying a bracelet) crosses the perimeter, a bracelet-crossing indication will be generated by all nodes n_i where the following statement is true:

$$(\boldsymbol{r}_m \in S_i) AND (d_{mi} \leq R_i) AND (d_{mi} \leq R_m). \quad (30)$$

In that case, also, an intruder alert will be generated by all nodes n_j where the following statement is true:

$$(\boldsymbol{r}_m \in S_j) AND \left[(d_{mj} > R_j) OR (d_{mj} > R_m) \right] \quad (31)$$

Figure 5 shows a graphical representation of the influence of these parameters on the described surveillance algorithm. There are some issues that arise in the scenario described above, that lead to the conclusion that time synchronization of perimeter nodes could be highly beneficial. These issues are summarized as follows:

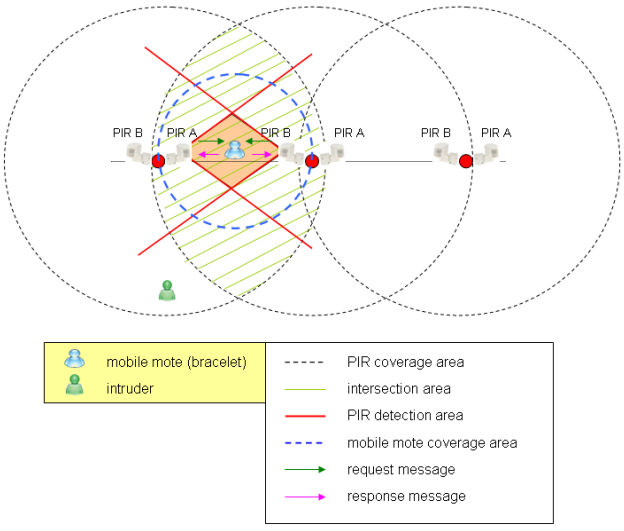

Figure 5. Influence of the different coverage areas of WSN perimeter nodes in the surveillance application algorithm.

- First of all, packets simultaneously generated in different nodes could invest different periods of time to reach the sink. In fact, since power consumption in a WSN is of the utmost importance, many communication protocols implement a low duty-cycle. The nodes are operative and ready to forward information during a small percentage of time in this cycle. Thus, if the packet must traverse several hops, the overall delay may be significant (e.g., tens, hundreds or even thousands of milliseconds).
- On the other hand, it is possible, depending on the combination among the coverage radio of the motes (R_i), the coverage radio of the mobile bracelets (R_m) and the PIR-detection areas (S_i), that two different nodes detect the same physical event (i.e., a particular crossing) and report it to the sink. Also, as shown in (30) and (31), the same crossing event could be notified by different nodes.
- All the above may lead to the reception of more than one warning to the sink (and to the server system beyond it) with a significant time offset but that actually correspond to the same crossing event. This is especially true if all warning messages do not follow the same path to the sink.

If the warning messages were timestamped by the originating motes (e.g., with the local time associated with the crossing event, which was locally reported to the perimeter agent) it would be much easier to detect and eliminate duplicated information, reducing the number of "false positives". Obviously, if different nodes timestamp their messages and if these timestamp values are compared later in the sink or in the server, it is necessary that those nodes have synchronized clocks with a certain tolerance, in order to decide if two event reports correspond to the same actual real-world event.

It is important to note that, although the detection range of the PIR sensors is not often configurable (and it makes difficult to avoid duplicated detections in some deployment scenarios), the radio coverage of a node usually is. Thus, the logical topology of the WSN may, under certain circumstances, be modified adjusting the transmission power of the nodes, which will reduce or increase the number of neighbors for each mote.

For instance, the increment of transmission power at perimeter nodes, and consequently R_i, leads to a growth in the number of neighbors of each node, reducing the associated graph diameter, D, of the surveillance WSN. For $k = 2$ (2-cycle, with four neighbors per node), $D = N/4$ if N is even, and $D = (N-1)/4$ if N is odd, while for $k = 4$ this diameter value halves, with subsequent effects in WSN synchronization, as shown in (28). The drawbacks of raising R_i are basically twofold: firstly, an increased transmission power implies higher energy consumption, a usually scarce resource in any WSN; secondly, large R_i may cause some inaccuracies when reporting crossings.

For instance, if there is an intruder crossing that is detected by node n_i, and R_i is too large, the corresponding question message may be received by a surrounding bracelet, which is not actually crossing the perimeter, but where the next statement is true:

$$(d_{mi} \le R_i) AND (d_{mi} \le R_m). \quad (32)$$

In that case, a bracelet-crossing event will be erroneously generated. In order to prevent this kind of collateral effects, if R_i is increased, the values of S_i (e.g., by a more precise physical orientation of the PIR sensors) and R_m should be carefully chosen. Thus, it will be possible to minimize the effect of false alarm incidences.

Next Section of this paper applies the results derived from the mathematical model described in previous sections to find adequate values for the WSN logical topology that ease and simplify the time synchronization process in this particular surveillance application scenario.

VII. Conditions of Synchronizability of the Surveillance WSN

In Section V, the mathematical results that link the eigenvalues of **L** and some overall network topological parameters have been shown, mainly in (27) and (28). Therefore, it is possible to apply those results to the surveillance WSN described in Section VI, in order to facilitate its synchronization. Conclusions are summarized as follows [1]:

- The number of nodes, N, must be reduced to a value as small as possible, but obviously the connectivity among node i and its two neighbors (nodes $i - 1$, $i + 1$) must be always assured to keep the surveillance perimeter properly closed.
- The WSN diameter, D, must be also reduced. This could be done increasing the coverage radio of every node i, e.g., to get connectivity with nodes $i - 2$ and $i + 2$ as well, which reduces D by 1/2. Further reductions of D can be obtained increasing the coverage radio of nodes even more, but it could be prohibitive in terms of energy consumption, as explained in Section VI.
- The maximum degree of nodes, $\boldsymbol{\Delta}$, should not be increased excessively. It leads to the conclusion that the reduction of network diameter D and the corresponding increase of the maximum degree $\boldsymbol{\Delta}$ must be balanced.
- The difference between minimum degree ($\boldsymbol{\delta}$) and maximum degree ($\boldsymbol{\Delta}$) must be as small as possible. It could be achieved if the physical distance among adjacent nodes is similar (and also if the coverage radio is equal for all nodes), to accomplish $\boldsymbol{\delta} = \boldsymbol{\Delta}$.

These generic conditions must be verified in specific cases. Since the Laplacian eigenvalues of the ring network selected to support surveillance applications are given by (15), it is possible to obtain an approximation to its maximum eigenvalue, γ_M. Although the values of i are integer, it will be assumed that $i \in \mathbb{R}$. Thus, the usual conditions of the maximum of a function can be imposed:

the first derivative of (15) with respect to *i* must be zero, and its second derivative, negative:

$$\frac{d\gamma_i}{di} = \frac{4\pi}{N}\sin\frac{2\pi(i-1)}{N} = 0, \quad (33)$$

$$\frac{d^2\gamma_i}{di^2} = \frac{8\pi^2}{N^2}\cos\frac{2\pi(i-1)}{N} < 0. \quad (34)$$

Both equations are satisfied by $i = 1 + N/2$. If this selected value of *i* is included in (15), eigenvalue γ_M is

$$\gamma_M \equiv \gamma_{\frac{N}{2}+1} = 2(1-\cos\pi) = 4. \quad (35)$$

And also, for $i = 2$, eigenvalue γ_2 is

$$\gamma_2 = 2(1-\cos\frac{2\pi}{N}). \quad (36)$$

The maximum eigenvalue $\gamma_{N/2+1}$, remains constant (independent of *N*), and algebraic connectivity, γ_2, trends to zero as *N* grows; the first derivative of (36) with respect to *N* is continuously decreasing, and trends to 0 as *N* grows, as well:

$$\frac{d\gamma_2}{dN} = -\frac{4\pi}{N^2}\sin\frac{2\pi}{N}. \quad (37)$$

The quotient between $\gamma_{N/2+1}$ and γ_2 must be bounded, as it was shown in Section V; the application of (27) and (28) shows, respectively,

$$1 < \frac{\gamma_{\frac{N}{2}+1}}{\gamma_2} < \frac{N(N-1)}{2}. \quad (38)$$

The upper bound for this quotient is not convenient for time synchronization for large *N*, since it grows with *N* at quadratic rate.

The above analysis can be extended to *k*-cycles, which gives similar results. Figure 6 shows, from (16), the dependence of *k*-cycles maximum eigenvalues, γ_M, with respect to the network number of nodes, *N*, for $k = \{1, 2, 3, 4\}$. These maximum eigenvalues grow with *k*, and they reach a steady value as *N* grows. In fact, γ_M only gets the maximum value given in (35) for *N* even. As a consequence of the previous assumption made, i.e., $i \in \mathbb{R}$, Figure 6 shows that values of γ_M are not strictly constant, although they trend, for large *N*, to the maximum value given in (35).

Figure 7 shows, from (16), the dependence of *k*-cycles algebraic connectivity, γ_2, also called first nonzero eigenvalue (FNZE), with respect to *N*, for $k = \{1, 2, 3, 4\}$. In all cases, FNZE trends to zero as *N* grows, which is not suitable for WSN synchronization. Finally, Figure 8 shows, from (16) and (38), the spectral bounds for the quotient $\gamma_{N/2+1}/\gamma_2$ in a ring network, with $k = 1$, as functions of *N*. The increasing upper bound for large *N* is not favorable for time synchronization, either.

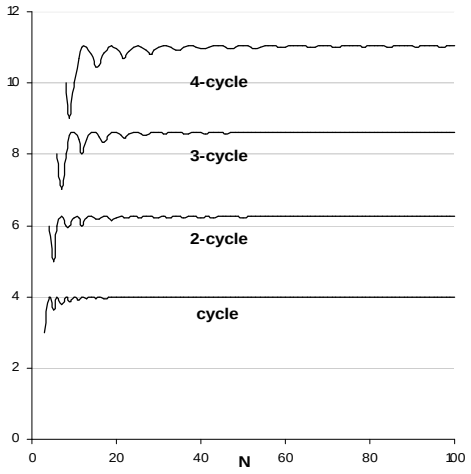

Figure 6. Maximum eigenvalues for *k*-cycles, γ_M, with $k=\{1,2,3,4\}$, as functions of the number of network nodes, *N*. These eigenvalues grow with *k*, and they stabilize for N large.

Although the convergence of the synchronization is initially guaranteed for WSN with ring topology, as it has been shown in Section IV, it can be concluded that this kind of network topology is not a good candidate for time synchronization, except for a reduced number of nodes. The increase of network degree, by the extension of coverage radio in network nodes, does not suppose a valuable help, and also it leads to a significant increment of power consumption. Next Section explores the validity of these theoretical results with the application of various synchronization protocols.

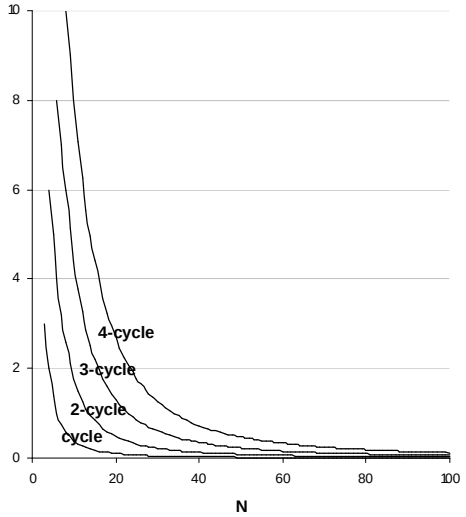

Figure 7. Algebraic connectivity, γ_2, or first nonzero eigenvalue (FNZE), for *k*-cycles, with $k=\{1,2,3,4\}$, as a function of the number of network nodes, *N*. In all cases, FNZE trends to zero as *N* grows.

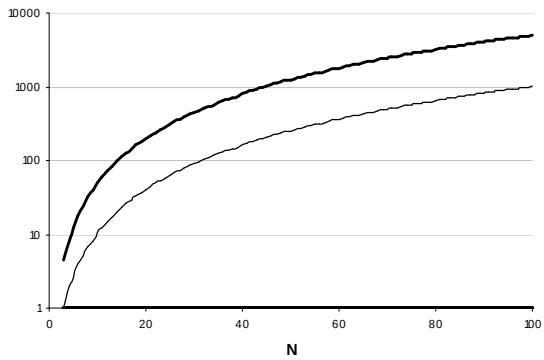

Figure 8. Spectral bounds for $\gamma_{N/2+1}/\gamma_2$ (bold lines) for a WSN with ring topology (cycle, with $k = 1$), as functions of N, number of network nodes. The curve $\gamma_{N/2+1}/\gamma_2$ remains bounded between 1 and $N(N-1)/2$. The increasing upper bound, for large N, is not adequate for time synchronization.

VIII. PERFORMANCE OF SYNCHRONIZATION PROTOCOLS IN THE SURVEILLANCE WSN

This Section explores the application and performance of various synchronization algorithms in the surveillance WSN with ring topology. The simulations will be applied to a WSN with a maximum of $N = 100$ nodes. The initial local clock times are randomly chosen, and the initial maximum offset between each pair of nodes is set up to one second. Figure 9 shows a typical distribution of the initial local clocks offset, with respect to the local clock of sink node, which will be chosen as the master clock in some synchronization algorithms. The unavoidable delay caused by transmission of messages among neighbor nodes and internal processing tasks is supposed constant. All the local clocks have the same angular frequency, and the effects of clock drift and skew are supposed to be negligible with respect to clock frequency during the synchronization stage. This last assumption is reasonable since the clock accuracy is limited. This simplified scenario, which can be further extended, can prove the suitability of different synchronization techniques applied to ideal situations, without the appearance of nondeterministic effects.

Some different synchronization algorithms have been tested. They can be divided in two types: the algorithms that rely on a distributed diffusion and adjustment of local clock values among adjacent nodes, following the time varying consensus model described in Section IV, and the algorithms based on a master clock time reference forwarded to all WSN nodes. In such cases, the synchronization is acquired in a progressive way, after a certain number of synchronization rounds. It is assumed, also, that the elapsed time between consecutive synchronization rounds is constant. The main goal of this Section is to identify the synchronization methods that minimize the number of synchronization steps.

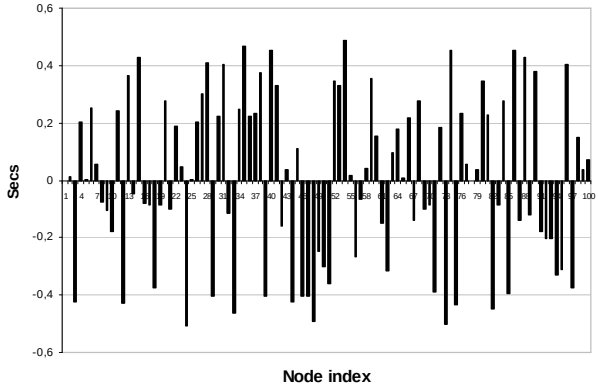

Figure 9. Initial local clocks offset (in seconds) for a network with $N = 100$ nodes. Initial offsets are relative to the master clock time of sink node. The initial local clock values are randomly chosen, with a maximum dispersion of 1 second among them.

A. Synchronization by distributed diffusion

Following the principles of the consensus dynamics model, shown in Section IV, the first synchronization method to test will be based on the exchange of local clock values among adjacent nodes. An initial broadcast message from the sink node can start the synchronization process. Immediately after the reception of this message, each node sends a message to its neighbors, containing its local clock time value.

Figure 10 shows this exchange process. The node i receives the clock values x_{i+1} and x_{i-1}. Since this reception is not simultaneous, let $\boldsymbol{\varepsilon}$ be this temporal difference. The packet transmission delay between nodes is $\boldsymbol{\mu}$. Assuming that x_{i+1} and x_{i-1} has been received at the same period of time T (elapsed time between two consecutive synchronization rounds), it could be considered that the contribution of $\boldsymbol{\varepsilon}$ and $\boldsymbol{\mu}$, are negligible (i.e., $T >> \boldsymbol{\varepsilon}$ and $T >> \boldsymbol{\mu}$) .

Once the nodes have received and recorded these values, each node compares its local clock time, x_i, and the timestamps received by its neighbors, x_{i+1} and x_{i-1}. Subsequently, the node adjusts its local clock with the average value from the local time x_i and the received values, x_{i+1} and x_{i-1}. Let us explore the synchronization convergence properties of this synchronization algorithm. Each synchronization round can be expressed as

$$x_{i,n+1} = \frac{1}{3}x_{in} + \frac{1}{3}\sum_{j=1}^{N} A_{ij}x_{jn}. \qquad (39)$$

From the definition of laplacian matrix components given in (14), $A_{ij} = \delta_{ij}D_{ij} - L_{ij}$,

$$x_{i,n+1} = \frac{1}{3}x_{in} + \frac{1}{3}\sum_{j=1}^{N} (\delta_{ij}D_{ij} - L_{ij})x_{jn}. \qquad (40)$$

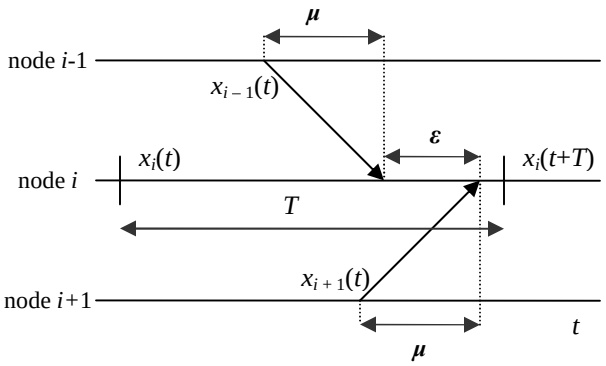

Figure 10. Exchange of local clock values among adjacent nodes. The reception of x_{i-1}, x_{i+1} by node i is supposed to take place into the same period of time, T, interval of elapsed time between two consecutive synchronization rounds .

Rearranging the second member terms of (40),

$$x_{i,n+1} = x_{in} - \frac{1}{3}\sum_{j=1}^{N} L_{ij} x_{jn}, \tag{41}$$

$$\Delta x_{in} = -\frac{1}{3}\sum_{j=1}^{N} L_{ij} x_{jn}. \tag{42}$$

And dividing for $\Delta t \equiv T$, the elapsed period of time between two consecutive synchronization rounds,

$$\frac{\Delta x_{in}}{\Delta t} = -\frac{1}{3\Delta t}\sum_{j=1}^{N} L_{ij} x_{jn} \approx -\frac{1}{3T}\sum_{j=1}^{N} L_{ij} x_{jn}. \tag{43}$$

Equation (43) can be expressed in vectorial form, as

$$\frac{\Delta \boldsymbol{x}_n}{\Delta t} = -\frac{1}{3T}\mathbf{L}\boldsymbol{x}_n. \tag{44}$$

So, it is proved that the synchronization method chosen, from the average values of local clocks of neighbors, follows the consensus dynamics model expressed in (19). This result can be easily extended for a regular k-cycle; the average time value of local clock $x_i(t)$ is calculated from its $2k$ neighbors. In that case, (44) can be generalized as

$$\frac{d\boldsymbol{x}}{dt} = -\frac{1}{(k+1)T}\mathbf{L}\boldsymbol{x}(t). \tag{45}$$

The coupling strength is equal to $[(k + 1)mT]^{-1}$. Adding the increment of local clocks with time, Figure 11 shows the convergence of this algorithm, for ring networks with different number of nodes, with a random initial distribution of local clocks offset similar to the distribution shown in Figure 9. In general, the time to get the synchronization trends to grow with N, but it depends, also, on the initial relative offset between local clocks. The individual evolution of local clock values follows a similar pattern to those shown in Figure 4 (time varying consensus dynamics).

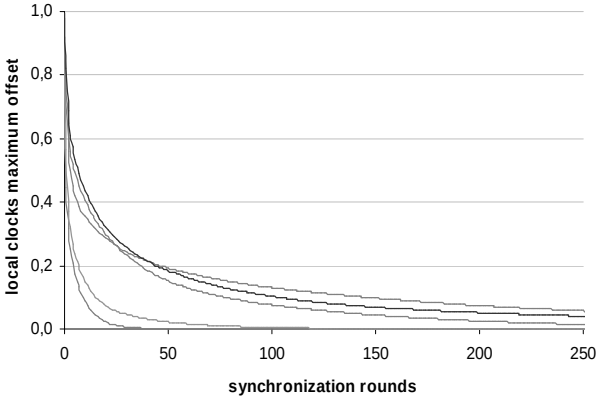

Figure 11. Evolution of maximum offset between local clocks, as a function of the synchronization rounds. Synchronization is driven by the time average value from adjacent nodes, x_{i-1}, x_i, and x_{i+1}, for ring networks with different N values, from $N = 10$ to $N = 100$. As N grows, synchronization trends to slow down.

The above synchronization algorithm does not consider a fundamental constraint in time synchronization: the local clocks should not run backwards [15]. To avoid this undesirable effect, if the time average value from x_{i-1}, x_i, and x_{i+1} is lower than the local time x_i, it will not be considered. Then, the synchronization process is given by

$$x_{i,n+1} \leftarrow \max\left(\frac{x_{in} + x_{i-1,n} + x_{i+1,n}}{3}, x_{in}\right). \tag{46}$$

Figure 12 shows the performance of this synchronization algorithm variant. Its performance is similar to the previous algorithm, but the reduction rate of local clocks relative offset is worse.

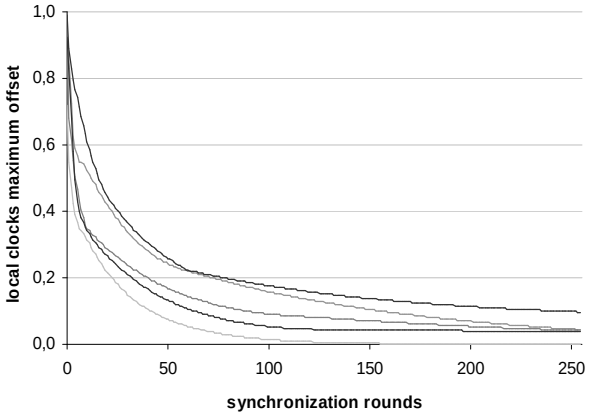

Figure 12. Evolution of maximum offset between local clocks, as a function of the synchronization rounds. Synchronization is driven by the time average value from adjacent nodes, x_{i-1}, x_i, and x_{i+1}, if the average value is greater than x_i, for ring networks with different N values, from $N = 10$ to $N = 100$. Although the graph is similar to the previous one, the performance of the algorithm is worse.

If the synchronization process was driven by the maximum time value of the neighbor local clocks, it seems plausible that the synchronization would be faster, since in all the synchronization rounds, the maximum value among x_{i-1}, x_i, and x_{i+1} is expanded towards two nodes:

$$x_{i,n+1} \leftarrow \max\{x_{in}, x_{i-1,n}, x_{i+1,n}\}. \quad (47)$$

Figure 13 shows the performance of this synchronization algorithm, for ring networks with different number of nodes, from N = 10 to 100, and initial local clocks offset randomly chosen. The synchronization process will be always finished after $N/2$ synchronization rounds, for N even, and after $(N - 1)/2$ rounds, for N odd. Figure 14 shows the same performance, for a ring network with N = 100 nodes and different initial local clock times. These results prove that this synchronization method is better than the previous diffusion algorithms, expressed in (41) and (46). The most advanced clock guides the whole synchronization process, which could be inappropriate for some applications. However, for the surveillance application purposes, it is preferable a fast synchronization.

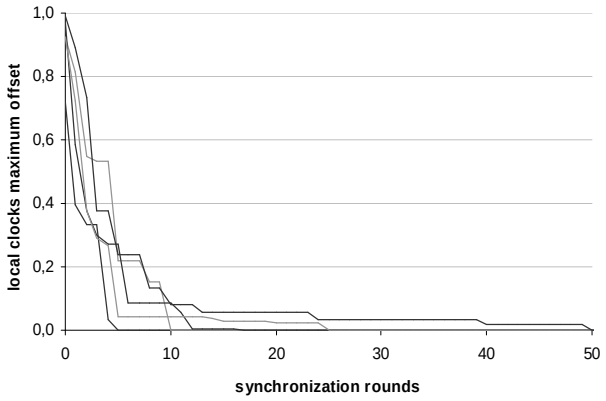

Figure 13. Maximum offset between local clocks. Synchronization driven by the time maximum value from adjacent nodes, x_{i-1}, x_i, and x_{i+1}, for ring networks with different N values, from N = 10 to N = 100. The synchronization is always reached after $(N-1)/2$ or $N/2$ synchronization rounds, for N odd or even, respectively.

B. Synchronization by a master clock reference

Another approach to the network synchronization can be driven by the periodic diffusion of a message containing a master clock reference, t_M, which is chosen as the local clock time of the sink node, n_1, in a similar way that the proposals included in [20][27][28]. It is assumed that the period of local clocks is larger than the message round trip time between adjacent nodes. The reference timestamp is sent sequentially from node 1 to node N:

$$n_1 \rightarrow n_2 \rightarrow \ldots \rightarrow n_N \rightarrow n_1.$$

Each node keeps a record of t_M, and also it relays the master time reference, t_M. It records the local timestamp, t_{li}, associated with the reception of t_M, as well. Once the message path is finished, n_1 sends a new message containing its local timestamp, t_E, associated with the reception of the initial message containing t_M. With these two values of time it is possible to estimate the global network round trip time between adjacent nodes, i.e., $(t_E - t_M)/N$.

Since each node knows its index i in the relay sequence, it will be able to adjust its local clock time, x_i, with the next expression:

$$x_i \leftarrow x_i - t_{li} + t_M + \frac{t_E - t_M}{N}(i-1). \quad (48)$$

Here, $x_i - t_{li}$ reflects the difference between the current local time at node i and the reception time of t_M. The term $t_M + (t_E - t_M)(i - 1)N^{-1}$ contains a correction due to the reception delay of t_M at node i, which is proportional to the position of node in the relay sequence, $i - 1$. To explore the convergence of this synchronization algorithm, x_i and t_{li} will be expressed from the initial time value, x_{0i},

$$x_i \leftarrow x_{0i} + \frac{t_E - t_M}{N}(i-1+N) - x_{0i} - \frac{t_E - t_M}{N}(i-1) +$$

$$+ t_M + \frac{t_E - t_M}{N}(i-1), \quad (49)$$

$$x_i \leftarrow t_M + \frac{t_E - t_M}{N}(N+i-1). \quad (50)$$

Thus, the adjusted time x_i depends on t_M, t_E, and the position of node i in the network. Each node adjusts its local clock in a different instant of time, according to its position in the synchronization sequence.

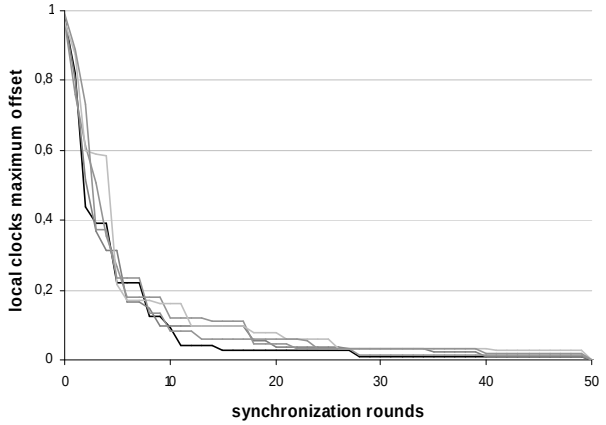

Figure 14. Performance of the synchronization protocol with the exchange of local timestamps from neighbor nodes and the selection of the maximum time value, for a WSN with ring topology with N = 100 nodes and different initial local clock times, which are randomly chosen with a maximum offset equal to 1 second. In all cases, synchonization time is reached in $N/2$ synchronization rounds.

Adding to (50) the correction of this difference, $(t_E - t_M)(N - i)N^{-1}$, all the x_i values are simultaneously equivalent:

$$x_i \leftarrow t_M + \frac{t_E - t_M}{N}(2N - 1). \quad (51)$$

The above process apparently reaches the synchronization in a fast way. However, as it was explained before, it is important to avoid adjustments of local clocks that could cause that local times could run backwards. So, (50) should be applied as

$$x_i \leftarrow \max\{x_i, t_M + \frac{t_E - t_M}{N}(N + i - 1)\}. \quad (52)$$

Figure 15 shows the local clocks offset with respect to the master clock after the application of (52). The resulting offset is caused by the above constraint: although maximum initial offset is reduced to the 50%, the synchronization has no effect on local clocks with an initial time advanced with respect to the master clock. Due to this constraint, more additional synchronization rounds cannot reduce this offset in a substantial way.

A further method could consist of the selection of the maximum value of local clocks. It can be initiated by the sink node; it transmits in sequence its local time value, and each node compare the received timestamp with its local time value, and it relays the maximum of these values. When the sequence is finished, the sink node receives the maximum value of local clocks, which will be chosen as the master clock reference. Then, the first synchronization method, expressed in (50), is applied. In that case, the synchronization time will be reached faster, as well, because all the nodes adjust their local time with the maximum value of local clocks.

Figure 16 allows to make a comparison of performances of some of the previous algorithms, in a WSN with ring topology with N = 100 nodes, after 100 synchronization rounds. The diffusion of a global time has a bad performance, due to the constraints discussed above. After these synchronization rounds, the reduction of the initial maximum offset is next to 50%.

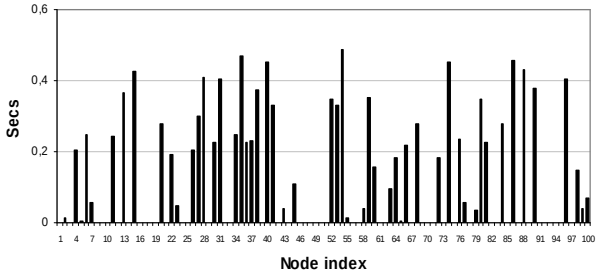

Figure 15. Synchronization driven by the transmission of a master clock reference. Local clock offset (in seconds) with respect to master clock time after one synchronization round. The reduction of the initial offset is approximately of 50%. The synchronization has no effect in local clocks advanced with respect to the master clock.

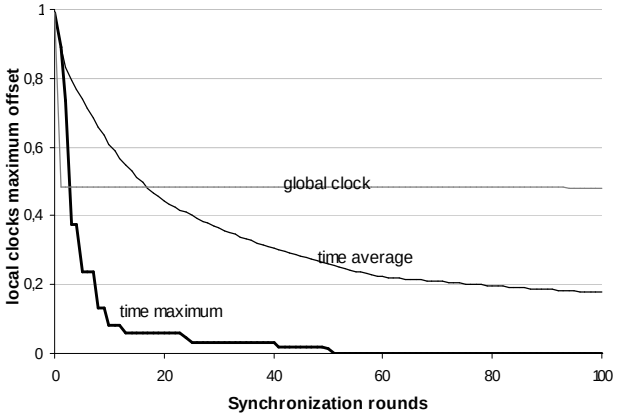

Figure 16. Performance of some synchronization algorithms described in Section VIII, in a WSN with ring topology with N= 100 nodes. The difussion of a global clock time across the network is the worst option, while the selection of the maximum time value from local clock time of neighbor nodes seems to be a more effective technique.

The selection of the average time value from neighbor nodes softly decreases the maximum offset between local clocks as the number of synchronization rounds grows; in that case, the reduction of the offset after the same number of synchronization rounds is about 80%. The best choice seems to be the selection of the maximum time value from neighbor nodes. The rough shape of the graphic line is due to the appearance of groups of local maximum times. These local values can remain unchanged during some synchronization rounds, until a greater time value gets its neighborhood.

IX. CONCLUSION AND FUTURE WORK

This paper has applied some well established results from System Dynamics and Algebraic Graph Theory to state the ease of the synchronization of a WSN with regular ring topology, which has been initially designed to support surveillance applications. It is assumed that local clocks of network nodes exhibit a linear behavior during the whole synchronization process, since the effects of clock drift and skew have been supposed negligible, due to the limited accuracy of local clocks. Furhermore, a constraint to prevent that clocks could run backwards had to be applied.

The synchronizability of the WSN is enhanced by means of a reduction of the number of network nodes, and also through the decrease of another overall topological parameters, as the network diameter and the maximum network degree. Apparently, as it is established by the theory, the selected topology by needs of the application domain is not a good initial candidate for time synchronization. However, the application of various synchronization algorithms, initially based on a distributed diffusion of local clock values and subsequently on the diffusion of a master clock reference, shows significant performance differences. The exchange of local timestamps among adjacent nodes, and the subsequent selection of the maximum of these values to adjust local clocks, seems to be an effective technique, as well as the diffusion of a master

clock reference, which is chosen as the maximum of local clock values.

As part of the future work, the above synchronization algorithms should be enriched with the addition of drift, skew and other nondeterministic effects. It is expected that the results obtained may guide the design of surveillance WSN and time synchronization protocols, and it is also foreseen to extract a set of more general rules to be extended to WSN with more complex topologies, and maybe designed for different purposes.

ACKNOWLEDGMENT

The research work described above has been partially funded by the European Commission, VI Framework Program, IST STREP Program, Action line IST-2005-2.5.3 (Embedded Systems), μSWN Project, code IST-034642. Also, the authors would like to thank Marta Zuazúa and Pedro Castillejo their initial contribution to the numerical simulations made.

REFERENCES

[1] José A. Sánchez Fernández, Ana B. García Hernando, José F. Martínez Ortega, and Lourdes López Santidrián, "Synchonization in a wireless sensor network designed for surveillance applications," Proc. Fifth International Conference in Wireless and Mobile Communications (ICWMC 2009), Cannes, France, Aug. 2009, IEEE Computer Society, pp. 369-372. doi: 10.1109/ICWMC.2009.68.

[2] Renato E. Mirollo and Stephen H. Strogatz, "Synchronization of pulse-coupled biological oscillators," SIAM J. Appl. Math., vol. 50, no. 6, Dec. 1990, pp.1645-1662.

[3] Duncan J. Watts and Steven H. Strogatz, "Collective dynamics of 'small-world' networks," Nature, vol. 393, June 1998, pp. 440-442. MacMillan Publishers Ltd., 1998.

[4] Yoshiki Kuramoto, Chemical Oscillations, Waves and Turbulences. Springer, 1984.

[5] Mauricio Barahona and L. M. Pecora, "Synchronization in small-world sytems," Phys. Rev. Letters, vol. 89, no. 5, July 2002, pp. 054101-1-054101-4.

[6] Louis M. Pecora, "Synchronization of oscillators in complex networks," Pramana – J. of Physics, vol. 70, no. 6, June 2008, pp. 1175-1198. Indian Academy of Sciences, 2008.

[7] Sergio Barbarossa and Francesco Celano, "Self-organizing sensor networks designed as a population of mutually coupled oscillators," Proc. IEEE Sixth Workshop on Signal Processing Advances in Wireless Communication (SPAWC 2005), New York, USA, June 2005, pp. 475-479.

[8] Sergio Barbarossa and Gesualdo Scutari, "Decentralized maximun-likelihood estimation for sensor networks composed of nonlinearly coupled dymanical systems," IEEE Transactions on Signal Processing, vol. 55, no. 7, July 2007, pp. 3456-3470.

[9] Sergio Barbarossa, Gesualdo Scutari, and Anantram Swami, "Achieving consensus in self-organizing wireless sensor networks: the impact of network topology in energy consumption," Proc. IEEE 32nd International Conference on Acoustics, Speech, and Signal Processing (ICASSP 2007), Honolulu, Hawaii, USA, April 2007, pp. II.841-II.844..

[10] Norman L. Biggs, Algebraic Graph Theory. Cambridge University Press, 1974.

[11] Allen J. Schwenk and Robin J. Wilson, "On the Eigenvalues of a Graph," in Selected Topics in Graph Theory, Lowell W. Beineke and Robin J. Wilson, Eds. Academic Press, 1978, pp. 307-336.

[12] Miroslav Fiedler, "Algebraic connectivity of graphs," Czechoslovak Mathematical Journal, vol. 23, no. 2, 1973, pp. 298-305. Institute of Mathematics, Acad. of Sc., Czech Republic.

[13] Bohan Mohar, "The Laplacian Spectrum of Graphs," in Graph Theory, Combinatorics, and Applications, vol. 2, Y. Alavi, G. Chartrand, O. R. Oellermann, and A. J. Schwenk, Eds. Wiley, 1991, pp. 871-898.

[14] Franesc Comellas and Silvia Gago, "Synchronizability of complex networks," Journal of Physics A: Mathematical and Theoretical, vol. 40, 2007, pp. 4483-4492. IOP Publishing, 2007.

[15] Bharath Sundararaman, Ugo Buy, and Ajay D. Kshemkalyani, "Clock synchronization for wireless sensor networks: a survey," Ad-Hoc Networks, 3(3). May 2005, pp. 281-323.

[16] Ya R. Faizulkhakov, "Time synchronization methods for wireless sensor networks: a survey," Programming and Computer Software, vol. 33, no. 4, 2007, pp. 214-226. Pleiades Publishing, Ltd. ISSN. 0361-7688.

[17] Brian M. Sadler and Ananthram Swami, "Synchronization in sensor networks: an overview," milcom, pp. 1-6. MILCOM 2006. ISBN: 1-4244-0617-X.

[18] Fikret Sivrikaya and Büllent Yener, "Time synchronization in sensor networks: a survey," IEEE Network, July/Aug. 2004, pp. 45-50.

[19] Kay Römer, Philipp Blum, and Lenart Meier, "Time Synchronization and Calibration in Wireless Sensor Networks," in Handbook of Sensor Networks: Algorithms and Architectures, I. Stojmenovic, Ed. Wiley and Sons, Oct. 2005, pp. 199-237.

[20] Qun Li and Daniela Rus, "Global clock synchronization in sensor networks," IEEE Transactions on Computers, vol. 55, no. 2, Feb. 2006, pp. 214-226, doi:10.1109/TC.2006.25.

[21] Osvaldo Simeone and Umberto Spagnolini, "Distributed time synchronization in wireless sensor networks with coupled discrete-time oscillators," EURASIP Journal on Wireless Communications and Networking, vol. 2007, pp. 1-13. Hindawi Publishing Corp. Article ID 57054, doi: 10.1155/2007/57004.

[22] Shyi-Long Lee, Yeung-Long Luo, Bruce E. Sagan, and Yeong-Nan Yeh, "Eigenvectors and eigenvalues of some special graphs. IV. Multilevel circulants," Int. J. of Quantum Chemistry, Vol. 41, 1992, pp. 105-116.

[23] Demetri P. Spanos, Reza Olfati-Saber, and Richard M. Murray, "Dynamic consensus on mobile networks," Proc. 16th International Federation of Automatic Control World Congress (IFAC 2006), Prague, Czech Republic, July 2005. Elsevier, 2006. ISBN: 978-0-08-0451084.

[24] Reza Olfati-Saber and Richard M. Murray, "Consensus problems in networks of agents with switching topology and time-delays," IEEE Transactions on Automatic Control, vol. 49, no. 9, Sept. 2004, pp. 1520-1532.

[25] Juan A. Almendral and Albert Díaz-Guilera, "Dynamical and spectral properties of complex networks," New Journal of Physics, vol. 9, (2007) 187, doi: 10.1088/1367-2630/9/6/187.

[26] μSWN Project website: http://www.uswn.eu. Date of last access: July, 20th 2010.

[27] Jeremy Elson, Lewis Girod, and Deborah Estrin, "Fine-grained network time synchronization using reference broadcasts," Proc. Fifth Symposium on Operating Systems Design and Implementation (OSDI 2002), Boston, Massachussets. Dec. 2002, Vol 36, pp. 147-163.

[28] Michael Mock, Reiner Frings, Edgar Nett, and Spiro Trikaliotis, "Continuous clock synchronization in wireless real-time applications," Proc. 19th IEEE Symposium on Reliable Distributed Systems (SRDS-00), Nuremberg, Germany, Oct. 2000, pp. 125–133..